The role of autophagy in high-fat diet induced insulin resistance of adipose tissues

Yovita Permata Budi [Equal first author, 1], **Yi-Hsuan Li** [Equal first author, 2], **Chien Huang** [2], **Mu-En Wang** [3], **Yi-Chun Lin** [4], **De-Shien Jong** [2], **Chih-Hsien Chiu** [Corresp., 2], **Yi-Fan Jiang** [Corresp. 1]

[1] Graduate Institute of Molecular and Comparative Pathobiology, National Taiwan University, Taipei, Taiwan

[2] Department of Animal Science and Technology, National Taiwan University, Taipei, Taiwan

[3] Department of Pathology, Duke University, North Carolina, Durham, United States

[4] Department of Animal Science, National Chung Hsing University, Taichung, Taichung, Taiwan

Corresponding Authors: Chih-Hsien Chiu, Yi-Fan Jiang
Email address: chiuchihhsien@ntu.edu.tw, yfjiang@ntu.edu.tw

Aims: Studies have observed changes in autophagic flux in the adipose tissue of type 2 diabetes patients with obesity. However, the role of autophagy in obesity-induced insulin resistance is unclear. We propose to confirm the effect of High-Fat Diet (HFD) on autophagy and insulin signaling transduction from adipose tissue to clarify whether altered autophagy-mediated HFD induces insulin resistance, and to elucidate the possible mechanisms in autophagy-regulated adipose insulin sensitivity.

Methods: C57BL/6 mice were fed with HFD to confirm the effect of HFD on autophagy and insulin signaling transduction from adipose tissue. Differentiated 3T3-L1 adipocytes were treated with Free Fatty Acids (FFAs) and Bafilomycin A1 to determine the autophagic flux. Chloroquine (CQ) was locally injected into mouse epididymal adipose and 3T3-L1 adipocytes to evaluate the role of autophagy in insulin signaling transduction.

Results: The HFD treatment resulted in a significant increase in SQSTM1/p62, Rubicon expression, and C/EBP Homologous Protein (CHOP) expression, yet the insulin capability to induce Akt (Ser473) and GSK3β (Ser9) phosphorylation were reduced. PHLPP1 and PTEN remain unchanged after CQ injection. In differentiated 3T3-L1 adipocytes treated with CQ, although the amount of phospho-Akt stimulated by insulin in the CQ-treated group was significantly lower, CHOP expressions and cleaved caspase-3 were increased and Bafilomycin A1 induced less accumulation of LC3-II protein.

Conclusion: Long-term high-fat diet promotes insulin resistance, late-stage autophagy inhibition, ER stress, and apoptosis in adipose tissue. Autophagy suppression does not affect insulin signaling transduction via phosphatase expression but indirectly causes insulin resistance through ER stress or apoptosis.

1 **Research Article**

2 Title: The Role of Autophagy in High-Fat Diet Induced 3 Insulin Resistance of Adipose Tissues

4

5 **Authors names and affiliations:**

6 Yovita Permata Budi[1], Yi-Hsuan Li[2], Chien Huang[2], Mu-En Wang[3], Yi-Chun Lin[4], De-Shien

7 Jong[2], Chih-Hsien Chiu[2*], Yi-Fan Jiang[1*]

8 [1] Graduate Institute of Molecular and Comparative Pathobiology, School of Veterinary

9 Medicine, National Taiwan University, Taipei, Taiwan.

10 [2] Department of Animal Science and Technology, National Taiwan University, Taipei, Taiwan.

11 [3] Department of Pathology, Duke University School of Medicine, Duke University, Durham,

12 North Carolina, United States.

13 [4] Department of Animal Science, National Chung Hsing University, Taichung, Taiwan.

14

15 [*]Corresponding Author: Chih-Hsien Chiu and Yi-Fan Jiang

16 Mailing address: Rm. 104-1, No.1, Sec. 4, Roosevelt Road, Taipei City 10617, Taiwan

17 Email: chiuchihhsien@ntu.edu.tw / yfjiang@ntu.edu.tw

Abstract

Aims: Studies have observed changes in autophagic flux in the adipose tissue of type 2 diabetes patients with obesity. However, the role of autophagy in obesity-induced insulin resistance is unclear. We propose to confirm the effect of High-Fat Diet (HFD) on autophagy and insulin signaling transduction from adipose tissue to clarify whether altered autophagy-mediated HFD induces insulin resistance, and to elucidate the possible mechanisms in autophagy-regulated adipose insulin sensitivity.

Methods: C57BL/6 mice were fed with HFD to confirm the effect of HFD on autophagy and insulin signaling transduction from adipose tissue. Differentiated 3T3-L1 adipocytes were treated with Free Fatty Acids (FFAs) and Bafilomycin A1 to determine the autophagic flux. Chloroquine (CQ) was locally injected into mouse epididymal adipose and 3T3-L1 adipocytes to evaluate the role of autophagy in insulin signaling transduction.

Results: The HFD treatment resulted in a significant increase in SQSTM1/p62, Rubicon expression, and C/EBP Homologous Protein (CHOP) expression, yet the insulin capability to induce Akt (Ser473) and GSK3β (Ser9) phosphorylation were reduced. PHLPP1 and PTEN remain unchanged after CQ injection. In differentiated 3T3-L1 adipocytes treated with CQ, although the amount of phospho-Akt stimulated by insulin in the CQ-treated group was significantly lower, CHOP expressions and cleaved caspase-3 were increased and Bafilomycin A1 induced less accumulation of LC3-II protein.

Conclusion: Long-term high-fat diet promotes insulin resistance, late-stage autophagy inhibition, ER stress, and apoptosis in adipose tissue. Autophagy suppression does not affect insulin signaling transduction via phosphatase expression but indirectly causes insulin resistance through ER stress or apoptosis.

Introduction

Although studies show that interaction of genetic and lifestyle factors cause type 2 diabetes (T2D), approximately 90% of people with T2D are overweight or obese [1]. Adipocyte hypertrophy in obesity will induce the impairment of insulin sensitivity and the overexpression of some inflammatory cytokines that make the adipocyte dysfunctional. The pathway begins with the activation of the insulin receptor tyrosine kinase (IR) by insulin, which phosphorylates and recruits different substrate adaptors such as the Insulin Receptor Substrate (IRS) family of proteins. Tyrosine phosphorylated IRS then displays binding sites for numerous signaling partners. Among them, PI3K has a significant role in insulin function, mainly via the activation of the Akt/PKB and the PKC cascades. Activated Akt induces glycogen synthesis by inhibiting GSK-3, protein synthesis via mTOR and downstream elements, and cell survival by inhibiting several pro-apoptotic agents. Akt phosphorylates and directly inhibits FoxO transcription factors. Inactivation of the receptor responses has been reported as the underlying cause of impaired insulin action.[1] PHLPP directly dephosphorylates AKT at its hydrophobic motif (Ser473). Additionally, mutations in PTEN have been reported to cause insulin resistance and obesity.[2] NHERF1 binds directly to PTEN and PHLPP1/2 via PDZ domain and scaffolds ternary complexes at the membrane to suppress the activation of the PI3K–AKT pathway.[3]

Recent studies have indicated extracellular disturbances, such as excess nutrient inflammation or hyperinsulinemia, cause intracellular stress in adipose tissues, which may damage these cells' ability to perform standard metabolic actions on insulin.[4] Concerning these intracellular stresses, some studies have identified autophagy as playing a vital role in regulation. Yin et al.[5] showed that ER stress might cause autophagy activation in adipocytes and thus lead to adaptive responses to extracellular disturbances[6], alleviating insulin resistance deterioration.

During autophagosome biogenesis in macroautophagy, two ubiquitin-like systems, LC3 processing and Atg5-Atg12 conjugation, are associated with expanding the phagophore membrane. [7] As for LC3, it is located on the membrane after post-translational modifications. The C-terminal end of the cytosolic form LC3-I is cleaved by Atg4, which is then activated by Atg7 and transferred to Atg3. Finally, a phosphatidylethanolamine (PE) will be conjugated to LC3-I to form LC3-II by Atg3.[8,9] As for the Atg5-Atg12-Atg16 complex system, it promotes the formation of LC3-II,[10] which, in addition to participating in autophagosome formation, also has the function of recognizing autophagic cargos. LC3-II acts as a receptor to interact with the adaptor on the targets to promote their uptake and degradation. One of the best-characterized adaptor molecules is p62/SQSTM1, a multifunctional adaptor that enables the turnover of ubiquitinated substrates.[11] After expanding phagophore membrane and cargo engulfment, mature autophagosome fuses with lysosome form autolysosome for cargo degradation.[12]

However, all of the above processes presupposes that the autophagy is still normal in the cells, but in the study of Soussi et al.,[13] the autophagy in adipocytes from obese patients may be damaged. The connection between impaired autophagy and insulin resistance was observed by Guo et al.[14] who showed that Atg7 knockdown in 3T3-L1 adipocytes caused a reduction in the phosphorylation capacity of both the insulin receptor β subunit and IRS-1 stimulated by insulin. Moreover, Cai et al.[15] also found that Akt wasn't activated by insulin in the white adipose tissue in a AdiAtg3KO mouse model, indicating that early-stage inhibition autophagy accelerated the decline in insulin sensitivity. However, the physiological function of damaged autophagy in adipose is unclear, including its role played in insulin resistance development. Therefore, this study was designed to confirm the effect of HFD on autophagy and insulin signaling transduction from adipose tissue. We then clarified whether altered autophagy-mediated HFD induces insulin

resistance. Afterward, we elucidated the possible mechanisms in autophagy-regulated adipose insulin sensitivity.

Materials & Methods

Animal

In this study, 8-week-old male C57BL/6 mice (obtained from the Laboratory Animal Center, College of Medicine, National Taiwan University) were housed at 25 ± 2°C, with an approximate 50-60% relative humidity and 12-hour light/12-hour dark cycle. Diets and water are freely accessed. Mice were acclimated for one month before the treatments started and placed in the cage according to their experimental group. Each cage contained 4-6 mice and was provided with enrichment (i.e. plastic tube, shredded paper, etc.). The cage will be cleaned and checked every week. After the treatment, the mice were anesthetized with 2.5% avertin (0.15 mL/10 g) through intraperitoneal injection and sacrificed by cervical dislocation. All the operations on and the usage of animals followed the National Institutes of Health Guide for the Care and Use of Laboratory Animals (NIH Publications No.8023, advised 1978), and were approved by the National Taiwan University Institutional Animal Care and Use Committee (NTU105-EL-00178).

High-fat diet-induced T2D in mice

B6 mice were randomly grouped to control diet (CTD) or high-fat diet (HFD) groups for 8 (n=4) and 16 weeks (n=6). The CTD and HFD were commercially available diets purchased from Research Diets (Product Number: D12450J and D12492). Before sacrifice at the 16th week, the mice were injected with insulin intraperitoneally for 30 minutes, and blood samples were collected from the orbital sinus. After blood sample collection, mice were sacrificed by cervical dislocation for tissue harvest.

Local chloroquine injection in epididymal adipose

The 12-week-old male C57BL/6 mice (n=4) were anesthetized with 2.5% avertin (0.15 mL/10 g) through intraperitoneal injection, followed by surgery. The identified epididymal adipose tissues were injected with a 2.5 mg/kg body weight dose of chloroquine (Sigma-Aldrich) in PBS or PBS alone (n=6). Mice were injected with insulin and sacrificed for tissue harvest at 10 and 14 hours after surgery.

Cell culture

3T3-L1 preadipocytes were purchased from Taiwan Bioresource Collection and Research Center (BCRC number: 60159). Cells were cultured in high glucose Dulbecco's modified eagle medium (DMEM) (D5648, Sigma-Aldrich; 12100046, Gibco) containing 10% newborn calf serum (16010159, New Zealand origin, Gibco), 1% penicillin-streptomycin (15140122, Gibco) and 2.5 g/L of $NaHCO_3$. Cells were maintained at 37℃ with 5% CO2 supplement. For cell maturation, 3T3-L1 preadipocytes were switched to a medium that contained 10% fetal bovine serum (10270106, South American origin, Gibco) when the cells were 70% confluent. The medium was also added with 1 μM dexamethasone, 0.5 mM methylisobutylxanthine (IBMX) and 1 μg/mL insulin. After 2 days of treatment, the cells were maintained in insulin-only treatment until they were fully differentiated. Bafilomycin (Tocris) and chloroquine were added to the culture medium for 4 and 24 hours in 3T3-L1 mature adipocytes and treated insulin 15 minutes before sampling. A hydrophobic fluorescent dye Nile red was used to observe the oil droplet accumulation in 3T3-L1 mature adipocytes after the treatment.

Protein sample preparation and Western blotting analysis

Adipose tissues were homogenized in Pierce IP Lysis Buffer (87787, ThermoFisher Scientific) containing complete EDTA-free Protease Inhibitor Cocktail (04693132001, Roche) and PhosSTOP (04906845001, Roche), and then centrifuged at 4℃, 16000×g for 20 minutes. Using

Pierce BCA Protein Assay Kit (23225, ThermoFisher Scientific), the samples were diluted and mixed with 4X Laemmli Sample Buffer (1610747, Bio-Rad) and 10 mM dithiothreitol (DTT) to give a final concentration of 2 μg/μL. As for the cell experiment, 3T3-L1 cells were rinsed once with PBS and collected directly in 1X Laemmli Sample Buffer plus 10 mM DTT after treatment. All harvested samples were immediately boiled at 98℃ for 10 minutes and then stored at -20℃.

Sodium dodecyl sulfate-polyacrylamide gel electrophoresis (SDS-PAGE) was conducted to separate proteins with different molecular weights, depending on the target protein's size. Precision Plus Protein Dual Color Standards (1610374, Bio-Rad) and protein samples were loaded into gel wells. Electrophoresis was performed using running buffer (25 mM Tris, 192 mM glycine, 0.1% SDS), and the voltages were set at 95 V and 110 V according to the sample during the stacking and resolving stages.

After electrophoresis, the separated proteins were transferred onto methanol-pre-wetted and transfer buffer-pre-equilibrated PVDF membrane (1620177, Bio-Rad) via the transfer buffer (25 mM Tris, 192 mM glycine, 20% methanol). The protein size was determined by either Trans-Blot Turbo Semi-dry Transfer System (170-4155, Bio-Rad) or Criterion Wet Transfer Blotter (170-4070, Bio-Rad). The proteins were transferred at 25 V constant voltage with 0.4 A for 35 minutes for semi-dry transfer. For wet transfer, gels were equilibrated in transfer buffer for 15 minutes to remove excessive SDS, and then the proteins were transferred at 70 V with 250 mA for 1 hour.

PVDF membranes were washed with methanol and stained with Ponceau S solution to visualize the transferred proteins. The fragment membranes cut at the target position were blocked with 5% non-fat milk in TBST and incubated with target protein-specific primary antibodies, which was diluted with 1% BSA in TBST overnight at 4℃. Membranes were washed with TBST three

156 times for 15, 10, and 10 minutes each and then incubated with the species-specific HRP-
157 conjugated secondary antibodies (1:2500 to 1:5000 diluted with 5% non-fat milk in TBST) for 1
158 hour at room temperature. Membranes were washed with TBST three times for 10, 5, and 5
159 minutes each and then the blotting images were visualized with Bio-Rad (1705061) and GE
160 (RPN2235) ECL substrates reagents using a Bio-Rad ChemiDoc Touch Imaging System.
161 Blotting quantification was performed using Bio-Rad Image Lab software. Table 1 presents
162 details about the antibodies.

163 **RNA extraction**

164 The RNA from mouse adipose tissues was extracted using TRIzol reagent (15596018,
165 ThermoFisher Scientific), which was homogenized at 4℃. Afterward, the lysates were added to
166 100 μL of chloroform and then shook for 15 seconds. After being incubated for 2-3 minutes at
167 room temperature, mixed lysates were centrifuged at 12,000×g for 15 minutes at 4℃. Thereafter,
168 the RNA-containing colorless upper aqueous phase was transferred to a new tube. The RNA was
169 precipitated by adding 250 μL of isopropyl alcohol, mixing the solution for 10 minutes at room
170 temperature, and then centrifuging it at 12,000×g for 10 minutes at 4℃ to spin down the RNA
171 pellets. After centrifugation, the supernatant was removed, and the pellets were washed twice
172 with 500 μL of 75% ethanol. Finally, the pellets were air-dried and dissolved in UltraPure
173 DNase/RNase-Free Distilled Water (10977023, ThermoFisher Scientific) by incubating them in
174 a water bath at 60℃. The RNA concentration was measured using a biophotometer.

175 **Reverse transcription and real-time PCR**

176 Total RNA was reverse transcribed to cDNA using a PrimeScripTM RT reagent Kit (RR037Q,
177 TaKaRa). First, 200-500 ng RNA was mixed with PrimeScript buffer, PrimeScript RT enzyme
178 mix I, 25 pmol oligo dT primer and 50 pmol random 6 mers, and then it was incubated at 37℃

for 30 minutes followed by inactivation of reverse transcriptase at 85℃ for 10 seconds. The cDNA products were diluted with DNase/RNase-free distilled water to give a final concentration of 10-20 ng/μL, and then stored at -20℃.

We used QuantStudio 3 System (Applied Biosystems) for quantitative real-time PCR (qPCR) analysis to measure the level of target gene mRNA expression. A 10-20 ng of cDNA template was mixed with Fast SYBR Green Master Mix (Applied Biosystems) and 0.4 μM target gene-specific primer pairs in a total volume of 10 μL. The reaction mixtures were transferred to well plates and then centrifuged. The samples were denatured for 20 seconds at 95℃ followed by 40 cycles of the PCR stage, with the denaturing step at 95℃ for 3 seconds and the annealing and extension step at 60℃ for 30 seconds. Finally, a melting curve analysis was conducted. The expression levels of ACTB were used as a loading control, and the gene-specific primer pairs are listed in Table 2.

Serum free fatty acid content analysis

To compare serum free fatty acid levels of the CTD-fed and HFD-fed mice, we used a commercial assay kit: the Free Fatty Acid Quantification Kit from BioVision (K612-100). Fifty μL of serum samples were mixed with 100 μL Reaction Mix. Then, the reactions were incubated at 37℃ for 30 minutes in the dark and the OD 570 nm value was measured. The sample readings were applied to the standard curve to obtain free fatty acid levels in the serum.

Statistical analysis

Each experiment was replicated at least three times and data were expressed as mean ± standard error of the mean (SEM). Data were analyzed by Student's t-test or one-way ANOVA followed by the least significant difference test (LSD) with Statistics Analysis System (Version 9.4, SAS Institute Inc.); $P < 0.05$ indicated statistically significant differences.

Results

HFD induces autophagy impairment, insulin resistance, endoplasmic reticulum (ER) stress, and apoptosis in adipose tissue

The mice treated with 8 weeks of HFD significantly increased SQSTM1/p62 and Rubicon expression, but the expression levels of LC3-II and Atg5 were unaltered (Figure 1B). Meanwhile, the mice treated with 16 weeks of HFD had a significantly increased expression of LC3-II and Atg5 (Figure 1D), which suggests that the late stage of autophagy might have been inhibited and that the autophagosomes accumulated in a large amount to elevate the expression of LC3-II on the autophagosome membrane. Further, p62 was degraded primarily by autophagy, and if the lysosomal degradation of autophagosome is blocked, an accumulation of p62 is expected, and so the expression of Rubicon also significantly increased.

There was no significant difference in serum total FFAs between the HFD and CTD groups at 8 and 16 weeks from the blood sample (Figure 1E). The western blotting data shows that insulin injection failed to induce Akt phosphorylation (Ser473) in adipose tissue from mice fed HFD for 16 weeks (Figure 1F). Meanwhile, we also observed the marker of endoplasmic reticulum (ER) stress, CHOP, was significantly increased. One of the key executioners of apoptosis, caspase-3, was activated as cleaved caspase-3 in adipose tissues from mice fed with HFD (Figure 1H).[16, 17]

We used differentiated 3T3-L1 adipocytes for FFA treatment to reinforce the conclusion that autophagy was inhibited in the in vivo experiment. This was done by treating 3T3-L1 cells with the mixture of 0.6 mM palmitic acid (PA) and 0.6 mM oleic acid (OA) for 48 hours. We observed that Bafilomycin A1 treatment given 4 hours before sampling induces less expression of LC3-II protein in FFA-treated cells than that in the BSA control group (Figures 2A,B).

Impaired late-stage autophagy may lead to insulin resistance indirectly by ER stress or apoptosis

To investigate whether autophagy inhibition can induce insulin resistance in a cell-autonomous manner, we conducted in vitro experiments using differentiated 3T3-L1 adipocytes. By treating differentiated 3T3-L1 with 40 μM of CQ for 24 hours, we first addressed whether the autophagy in 3T3-L1 cells was inhibited. After treatment with CQ, we observed increased LC3-II and SQSTM1/p62 protein levels in 3T3-L1 cells (Figures 3B, 3C). We found that phospho-Akt (Ser473) in the CQ-treated group was significantly lower than that in the control (Figure 3D).

Interestingly, our Western blotting data showed that CQ-treated adipocytes had significantly higher CHOP levels and cleaved caspase-3 than those in the control (Figure 3F), which echoed the in vivo experiment results observed in the adipose from mice fed with HFD. To further clarify whether insulin resistance was directly affected by autophagy inhibition or by concomitant ER stress or apoptosis, we excluded the effects of apoptosis on cells by reducing CQ concentrations. The protein levels in LC3-II in the treatment group were higher than those the control group, while the levels of SQSTM1/p62 were significantly increased at the concentrations of 20 and 30 μM when compared to those of the control group (Figures 4B, C).

Moreover, the expression of cleaved caspase-3 did not change (Figure 4D). Hence, we chose 20 μM dosage to determine if autophagy inhibition per se can induce insulin resistance; it did not influence insulin-stimulated Akt phosphorylation in 3T3-L (Figure 4F).

The correlation between the late-stage autophagy inhibition with insulin resistance in adipose tissue

The results indicate that 10 hours after CQ injection, the phosphorylation level induced by insulin was not significantly different from that of the control group (Figure 5B). However,

the capability of insulin to generate Akt (Ser473) and GSK3β (Ser9) phosphorylation was reduced 24 hours after CQ injection (Figures 5D, 5E).

Additionally, although the protein levels of SQSTM1/p62 and LC3-II were no difference between CQ-treated and control groups (Figure 6A and 6B), the LC3 mRNA expression was significantly decreased in adipose tissues with CQ injection (Figure 6C). These data suggested that at the 24-hour post-injection of CQ, the suppression of late stage autophagy may have feedback effect which resulted in reduced mRNA level of LC3.

The phosphorylation of insulin signaling blocked by autophagy is not associated with the expression of PHLPP1 and PTEN

After confirming that the inhibition of late-stage autophagy is related to the occurrence of insulin resistance, we further investigated the molecular mechanisms that may be involved. As it was previously reported that the expression of PHLPP1 is elevated in adipose tissue of obese patients and mice, which in turn leads to a decrease in phosphorylation of Akt and affected insulin sensitivity,[18] we first checked the protein level of PHLPP1 in mouse adipose treated with CQ. According to the Western blotting data, the CQ injection did not increase the expression of PHLPP1 compared to that in the control group. The amount of PTEN after CQ treatment was also not changed (Figure 7 B).

Discussion

Insulin resistance is considered one of the crucial factors in early-stage T2D development, which can cause metabolic dysfunction in tissues. As cellular functions that may be involved in insulin resistance, studies have pointed out that autophagy plays a critical role in the progression of T2D, which is related to the adaptive response to intracellular stress. In particular, Cai et al.[15] observed that autophagy ablation can damage the insulin signaling transduction in adipose

tissues. However, the role of autophagy in adipose function and the molecular mechanisms of how autophagy inhibition affects the insulin signaling pathway remain unclear.

HFD treatment for 8 weeks led to a blockade of late-stage autophagy in adipose, and the inhibition of autophagy was observed even at the 16th week (Figures 1A, B). Rubicon's increased expression was the prominent cause of suppression at the late stage, which was similar to the results of Tanaka et al.[19] and Wang et al.[20] in hepatocytes. Fatty acid-treated cells showed a significant decrease in autophagic flux (Figure 2), which doubly confirmed that autophagy was inhibited and is also consistent with the clinical findings of Soussi et al.[13] Meanwhile, endoplasmic reticulum (ER) stress and apoptosis was also identified in adipose tissue (Figure 1D). Studies have demonstrated that these are two effects of HFD, and Kawasaki et al.[21] further clarified that ER stress is induced by reactive oxygen species (ROS) generation and inflammatory cytokines. However, Feng et al.[22] showed that the inflammatory response doesn't cause apoptosis. Our study brings a new evidence that HFD causes late-stage autophagy suppression in adipose associated with Rubicon upregulation. At the same time, a series of complex reactions, including insulin resistance, ER stress, and apoptosis, also occurs.

The suppression of late-stage autophagy may damage insulin signaling transduction (Figure 5B). This might be associated with the time point of sampling, or that the local injection didn't allow the drug to spread throughout the tissue. Interestingly, the mRNA expression of LC3 in early-stage autophagy was reduced (Figure 6C), thus suggesting that the inhibition of late-stage autophagy may cause feedback to decrease the mRNA level of LC3 and subsequently to block the early-stage autophagy. According to previous studies, if the early-stage autophagy is sometime suppressed, insulin resistance may worsen.[14,15]

We hypothesized that some phosphatases could not be degraded because of the blocked autophagic degradation, which would increase their expression and hinder the cascade of phosphorylation events in the insulin signaling pathway. The protein levels of PH domain and leucine-rich repeat protein phosphatase 1 (PHLPP1) and protein-tyrosine phosphatase 1B (PTP1B), in adipose from obese mice or patients exhibit a significant increase compared to lean animals.[18,23] In this study, the amount of PHLPP1 didn't elevate as expected in the CQ-treated group but instead decreased significantly (Figure 7A). It shows that autophagy suppression didn't cause Akt phosphorylation to be restricted due to increased expression of PHLPP1; conversely, it reduced the protein level of PHLPP1. In this regard, we suppose that autophagy which mediated the degradation of Mir6981 was inhibited, thereby leading to the abundance of Mir6981 that mitigated the protein translation of PHLPP1.[24] In addition, there was no significant difference of phosphatase and tensin homolog (PTEN) between the CQ-treated and control group (Figure 4B). This indicates that PTEN was also not involved in the insulin signaling transduction blocked by autophagy inhibition. Hence, late-stage autophagy inhibition blocked the phosphorylation of downstream insulin signaling was independent of PHLPP1 and PTEN.

At a high dose (40 μM) of CQ, the insulin sensitivity in 3T3-L1 adipocytes was reduced and accompanied by ER stress and apoptosis (Figure 3), which was almost identical to the findings from the in vivo experiments. However, insulin signaling was still transduced normally in 3T3-L1 treated with CQ, thus suggesting that autophagy suppression may not directly contribute to insulin resistance. But it is also possible that the abnormality of the insulin signaling pathway did not occur at the time of sampling. After CQ treatment for 48 hours, the 3T3-L1 adipocytes developed insulin resistance as expected, but ER stress and apoptosis were also induced (Figure 4). These results strongly demonstrate that inhibition of late-stage

316 autophagy per se didn't directly cause insulin resistance in the adipocyte. Studies have indicated
317 that CQ blocks the fusion of autophagosome and lysosome, which leads to the accumulation of a
318 large number of damaged proteins in the cytoplasm and induces ER stress.; persistent ER stress
319 eventually results in cell death.[25] Moreover, van der Kallen et al.[26] showed that the relation of ER
320 stress with insulin resistance is more evident than its relation with apoptosis. In adipose, ER
321 stress triggers activation of c-Jun N-terminal kinase (JNK) through activated inositol requiring 1
322 alpha (IRE1α), thereby inhibiting serine phosphorylation of IRS1, and resulting in insulin
323 resistance.[27] In addition, adipocyte apoptosis contributes to macrophage infiltration into adipose
324 tissues, which increases the production of inflammatory cytokines. And these cytokines can
325 affect the insulin signaling, such as TNFα that also inhibits IRS1 phosphorylation.[28] In summary,
326 the suppression of late-stage autophagy caused by HFD may lead to a large accumulation of
327 impaired proteins in adipocytes, which in turn leads to ER stress and apoptosis. And the latter
328 two will eventually induce insulin resistance in adipose tissue.

329 ## Conclusions

330 A long-term high-fat diet promotes insulin resistance in adipose tissue and leads to the
331 increased protein levels of Rubicon, which blocks late-stage autophagy and is accompanied by
332 endoplasmic reticulum (ER) stress and apoptosis. Among these conditions, inhibition of late-
333 stage autophagy is clearly associated with a decrease in insulin sensitivity. However, autophagy
334 suppression does not affect the insulin signaling transduction via the pathway of PHLPP1 and
335 PTEN but instead causes insulin resistance indirectly through ER stress or the apoptosis
336 pathway.

337 ## Acknowledgements

338 This study was supported by grants from the Ministry of Science and Technology (109-2320-B-
339 002 -038 -MY3) (to Dr. Yi-Fan Jiang, National Taiwan University) and (106-2320-B-002-040-

MY3 and 109-2314-B-002-099-MY3) (to Dr. Chih-Hsien Chiu, National Taiwan University). The authors declare no conflicts of interest.

References

1. Copps KD, White MF. Regulation of insulin sensitivity by serine/threonine phosphorylation of insulin receptor substrate proteins IRS1 and IRS2. Diabetologia 2012; 55(10): 2565-2582. doi: 10.1007/s00125-012-2644-8

2. Pal A, Barber TM, Van de Bunt M et al. PTEN mutations as a cause of constitutive insulin sensitivity and obesity. N Engl J Med 2012; 367(11): 1002-1011. doi: 10.1056/NEJMoa1113966

3. Molina JR, Agarwal NK, Morales FC, et al. PTEN, NHERF1 and PHLPP form a tumor suppressor network that is disabled in glioblastoma. Oncogene 2012; 31(10): 1264-1274. doi:10.1038/onc.2011.324

4. Fazakerley DJ, Krycer JR, Kearney AL et al. Muscle and adipose tissue insulin resistance: malady without mechanism? J. Lipid Res 2019; 60(10): 1720-1732. doi: 10.1194/jlr.R087510

5. Yin J, Wang Y, Gu L et al. Palmitate induces endoplasmic reticulum stress and autophagy in mature adipocytes: Implications for apoptosis and inflammation. Int J Mol Med 2015; 35(4): 932-940. doi: 10.3892/ijmm.2015.2085

6. Zhou L, Zhang J, Fang Q et al. Autophagy-mediated insulin receptor down-regulation contributes to endoplasmic reticulum stress-induced insulin resistance. Mol Pharmacol 2009; 76(3): 596-603. doi: 10.1124/mol.109.057067

7. Yang Z, Klionsky DJ. Mammalian autophagy: Core molecular machinery and signaling regulation. Curr Opin Cell Biol 2009; 22(2): 124-131. doi: 10.1016/j.ceb.2009.11.014

8. Kabeya Y, Mizushima N, Yamamoto A et al. LC3, GABARAP and GATE16 localize to autophagosomal membrane depending on form-II formation. J Cell Sci 2004; 117: 2805-2812.

9. Hanada T, Noda NN, Satomi Y et al. The Atg12-Atg5 conjugate has a novel E3-like activity for protein lipidation in autophagy. J Biol Chem 2007; 282(52): 37298-302.

10. Romanov J, Walczak M, Ibiricu I et al. Mechanism and functions of membrane binding by the Atg5-Atg12/Atg16 complex during autophagosome formation. EMBO J 2012; 31(22): 4304-4317. doi: 10.1038/emboj.2012.278

11. Glick D, Barth S, Macleod KF. Autophagy: cellular and molecular mechanisms. J Pathol 2010; 221(1): 3-12. doi: 10.1002/path.2697.

12. Mizushima N. Autophagy: process and function. Genes Dev 2007; 21(22): 2861-73

13. Soussi H, Reggio S, Alili R et al. DAPK2 downregulation associates with attenuated adipocyte autophagic clearance in human obesity. Diabetes 2015; 64(10): 3452-3463. doi: 10.2337/db14-1933

14. Guo Q, Xu L, Li H et al. 4-PBA reverses autophagic dysfunction and improves insulin sensitivity in adipose tissue of obese mice via Akt/mTOR signaling. Biochem Biophys Res Commun 2017; 484(3): 529-535. doi: 10.1016/j.bbrc.2017.01.10616.

15. Cai J, Pires KM, Ferhat M et al. Autophagy ablation in adipocytes induces insulin resistance and reveals roles for lipid peroxide and Nrf2 signaling in adipose-liver crosstalk. Cell Rep 2018; 25 (7): 1708-1717.e5. doi: 10.1016/j.celrep.2018.10.040

16. Kadowaki H, Nishitoh H. Signaling pathways from the endoplasmic reticulum and their roles in disease. Genes (Basel) 2013; 4(3): 306-333. doi: 10.3390/genes4030306.

17. Crowley LC, Waterhouse NJ. Detecting cleaved caspase-3 in apoptotic cells by flow cytometry. *Cold Spring Harb Protoc* 2016; 2016(11). doi: 10.1101/pdb.prot087312.

18. Andreozzi, F, Procopio C, Greco A et al. Increased levels of the Akt-specific phosphatase PH domain leucine-rich repeat protein phosphatase (PHLPP)-1 in obese participants are associated with insulin resistance. Diabetologia 2011; 54(7): 1879-1887. doi: 10.1007/s00125-011-2116-6

19. Tanaka S, Hikita H, Tatsumi T et al. Rubicon inhibits autophagy and accelerates hepatocyte apoptosis and lipid accumulation in nonalcoholic fatty liver disease in mice. Hepatology 2016; 64(6): 1994-2014. doi: 10.1002/hep.28820

20. Wang ME, Singh BK, Hsu MC et al. Increasing dietary medium-chain fatty acid ratio mitigates high-fat diet induced non-alcoholic steatohepatitis by regulating autophagy. Sci Rep 2017; 7: 13999. doi:10.1038/s41598-017-14376-y

21. Kawasaki N, Asada R, Saito A et al. Obesity induced endoplasmic reticulum stress causes chronic inflammation in adipose tissue. Sci Rep 2012*;* 2: 799. doi: 10.1038/srep00799

22. Feng D, Tang Y, Kwon H et al. High-fat diet-induced adipocyte cell death occurs through a Cyclophilin D intrinsic signaling pathway independent of adipose tissue inflammation. Diabetes 2011; 60(8): 2134-2143. doi: 10.2337/db10-1411

23. Zabolotny JM, Kim YB, Welsh LA et al. Protein-tyrosine phosphatase 1B expression is induced by inflammation in vivo. J Biol Chem 2008; 283(21): 14230-14241. doi: 10.1074/jbc.M800061200

406 24. Peng M, Wang J, Tian Z et al. Autophagy-mediated Mir6981 degradation exhibits
407 CDKN1B promotion of PHLPP1 protein translation. Autophagy 2019; 15(9): 1523-1538.
408 doi: 10.1080/15548627.2019.1586254
409 25. Jia B, Xue Y, Yan X et al. Autophagy inhibitor chloroquine induces apoptosis of
410 cholangiocarcinoma cells via endoplasmic reticulum stress. Oncol Lett 2018; 16(3):
411 3509–3516. doi: 10.3892/ol.2018.9131
412 26. van der Kallen, CJH, van Greevenbroek MMJ, Stehouwer CDA et al. Endoplasmic
413 reticulum stress-induced apoptosis in the development of diabetes: Is there a role for
414 adipose tissue and liver? Apoptosis 2009; 14(2): 1424-1434. doi: 10.1007/s10495-009-
415 0400-4
416 27. Zhang K, Kaufman RJ. From endoplasmic-reticulum stress to the inflammatory response.
417 Nature 2008; 454(7203): 455-462. doi: 10.1038/nature07203
418 28. Alkhouri N, Gornicka A, Berk MP et al. Adipocyte apoptosis, a link between obesity,
419 insulin resistance, and hepatic steatosis. J Biol Chem 2010; 285(5): 3428-3438. doi:
420 10.1074/jbc.M109.074252
421

Figure 1

Altered autophagy in adipose tissues from mice fed with HFD

Altered autophagy, insulin resistance, and ER stress in adipose tissues from mice fed with 8- and 16-week HFD. The 12-week-old male B6 mice were fed with either the control diet or HFD for 8 weeks (A) and 16 weeks (B). T t he figure shows the immunoblots and the densitometric qua n tifications of SQSTM1/p62, LC3, Rubicon, and Atg5 expression by Western blotting. Values are mean ± SEM (n=4). The serum-free fatty acid levels between CTD-fed and HFD-fed mice were analyzed using a commercial assay kit (C). Values are mean ± SEM (8 weeks: n=4 and 16 weeks: n=6). n.s.: no significant difference. The phospho-Akt (Ser473) levels of adipose tissues from mice injected with or without insulin (0.5 IU/kg body weight I.P., 30 minutes) were analyzed at the 16th week using Western blotting (D). Values are mean ± SEM (n=6). Different letters are considered statistically significant difference by one-way ANOVA and least significant difference (LSD) test, $P < 0.05$. (E) Male B6 mice were fed with either the control diet or HFD for 16 weeks. The figure shows the immunoblots and the densitometric quantifications of CHOP and cleaved caspase-3 expression by Western blotting. Values are mean ± SEM (n=6). * indicates statistical significance, $P < 0.05$.

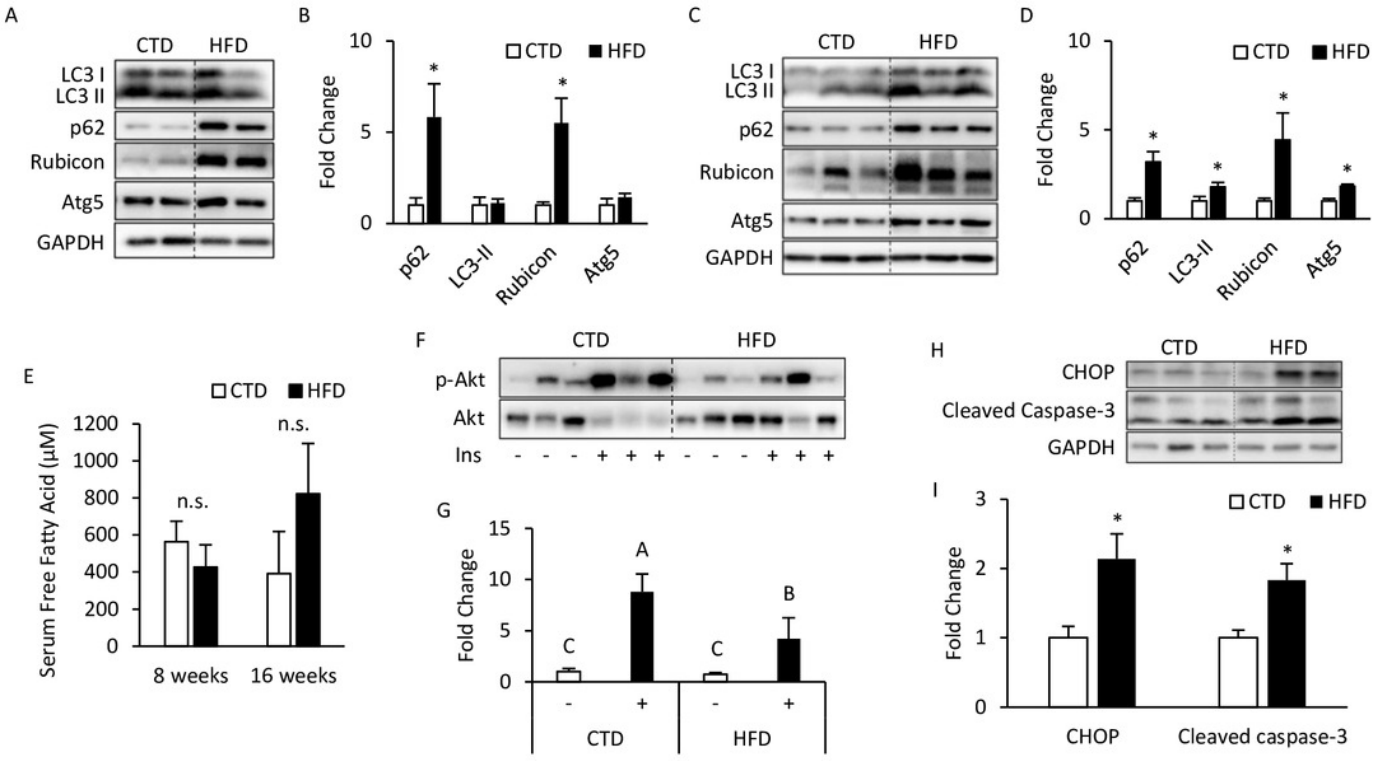
A
CTD
HFD
LC3 I
LC3 II
p62
Rubicon
Atg5
GAPDH
B
CTD
HFD
Fold Change
p62
LC3-II
Rubicon
Atg5
C
D
E
Serum Free Fatty Acid (μM)
n.s.
8 weeks
16 weeks
F
p-Akt
Akt
Ins
G
A
B
C
H
CHOP
Cleaved Caspase-3
I
Cleaved caspase-3

Figure 2

Free fatty acids (FFAs) impaired the autophagic flux in differentiated 3T3-L1 adipocytes

Free fatty acids (FFAs) impaired the autophagic flux in differentiated 3T3-L1 adipocytes. The Bafilomycin A1-induced LC3 II protein accumulation in 48-hour BSA- and FFA- (0.6 mM PA + 0.6 mM OA) loaded 3T3-L1 adipocytes were analyzed using Western blotting. The immunoblots, and calculated fold change of LC3 II protein levels were presented. For densitometric analyses, GAPDH was used as the loading control. Values are mean ± SEM (n=3). * indicates statistical significance, $P < 0.05$.

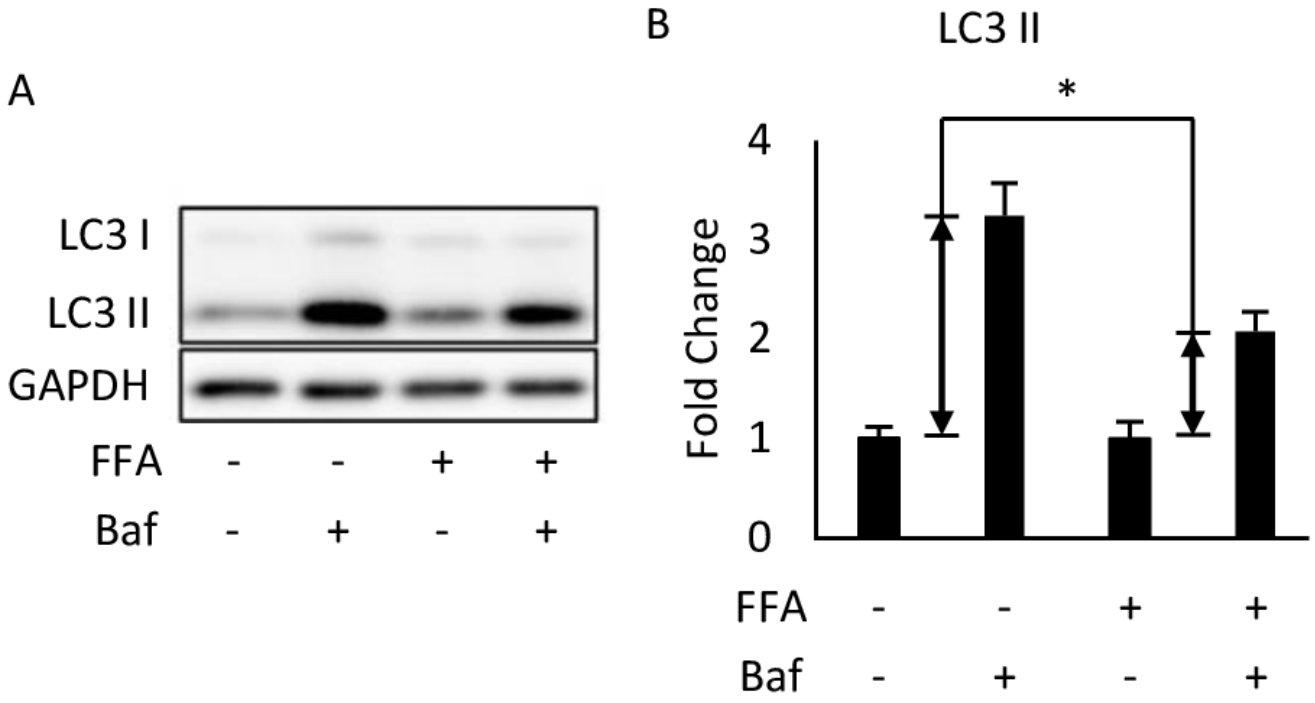

Figure 3

Autophagy inhibition, insulin resistance, ER stress and apoptosis were found in 3T3-L1 after CQ treatment for 24 hours

Autophagy inhibition, insulin resistance, ER stress and apoptosis were found in 3T3-L1 after CQ treatment for 24 hours. The differentiated 3T3-L1 adipocyte was treated with 40 μM CQ for 24 hours, and with 40 nM insulin for 15 minutes before sampling. SQSTM1/p62, LC3 and p-Akt/Akt immunoblots and densitometric quantifications (A). The differentiated 3T3-L1 adipocyte was treated with 40 μM CQ for 24 hours. CHOP and cleaved caspase-3 immunoblots and densitometric quantifications (E). For densitometric analyses of Western blotting data, GAPDH was used as the loading control. Values are mean ± SEM (n=3). Different letters are considered statistically significant difference by one-way ANOVA and least significant difference (LSD) test, $P < 0.05$.

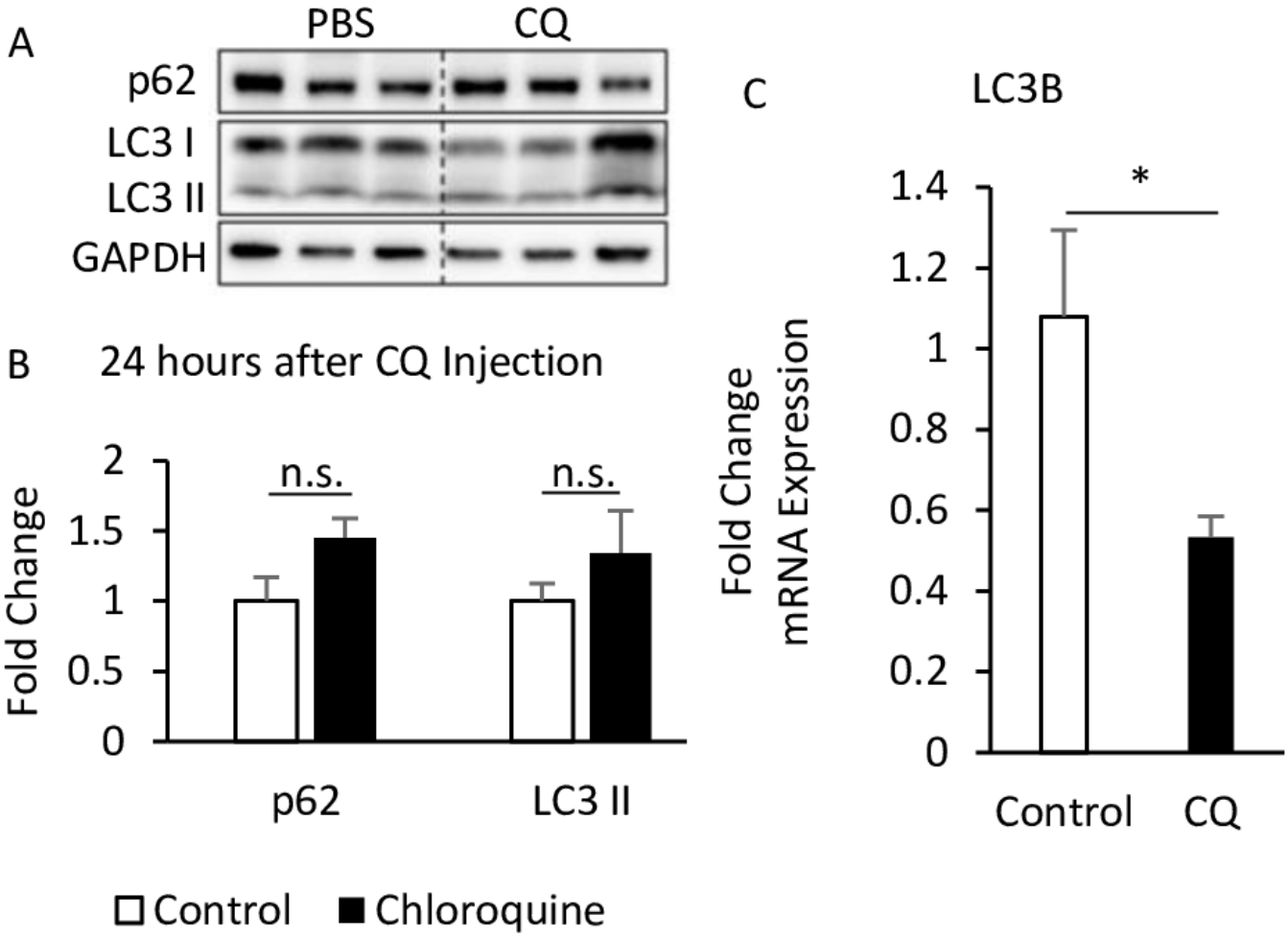
A
PBS
CQ
p62
LC3 I
LC3 II
GAPDH
B
24 hours after CQ Injection
Fold Change
2
1.5
1
0.5
0
n.s.
n.s.
p62
LC3 II
Control
Chloroquine
C
LC3B
Fold Change
mRNA Expression
1.4
1.2
1
0.8
0.6
0.4
0.2
0
*
Control
CQ

Figure 4

Dose-response experiment of CQ treatment in 3T3-L1 cells

Dose-response experiment of CQ treatment in 3T3-L1 cells and insulin resistance, ER stress, and apoptosis were observed in 3T3-L1 after 20 μM CQ treatment for 48 hours The differentiated 3T3-L1 adipocyte was treated with 10, 20, and 30 μM CQ, for 24 hours (A). The figure shows SQSTM1/p62 (B), LC3 (C), and cleaved caspase-3 (D) immunoblots and densitometric quantifications. The differentiated 3T3-L1 adipocyte was treated with 20 μM CQ for 24 hours and with 40 nM insulin for 15 minutes before sampling. The phospho-Akt (Ser473) and total Akt levels of 3T3-L1 adipocyte were analyzed using Western blotting (E,F). GAPDH was used as the loading control. Values are mean ± SEM (n=3). Different letters are considered statistically significant difference by one-way ANOVA and least significant difference (LSD) test, $P < 0.05$. n.s.: no significant difference.

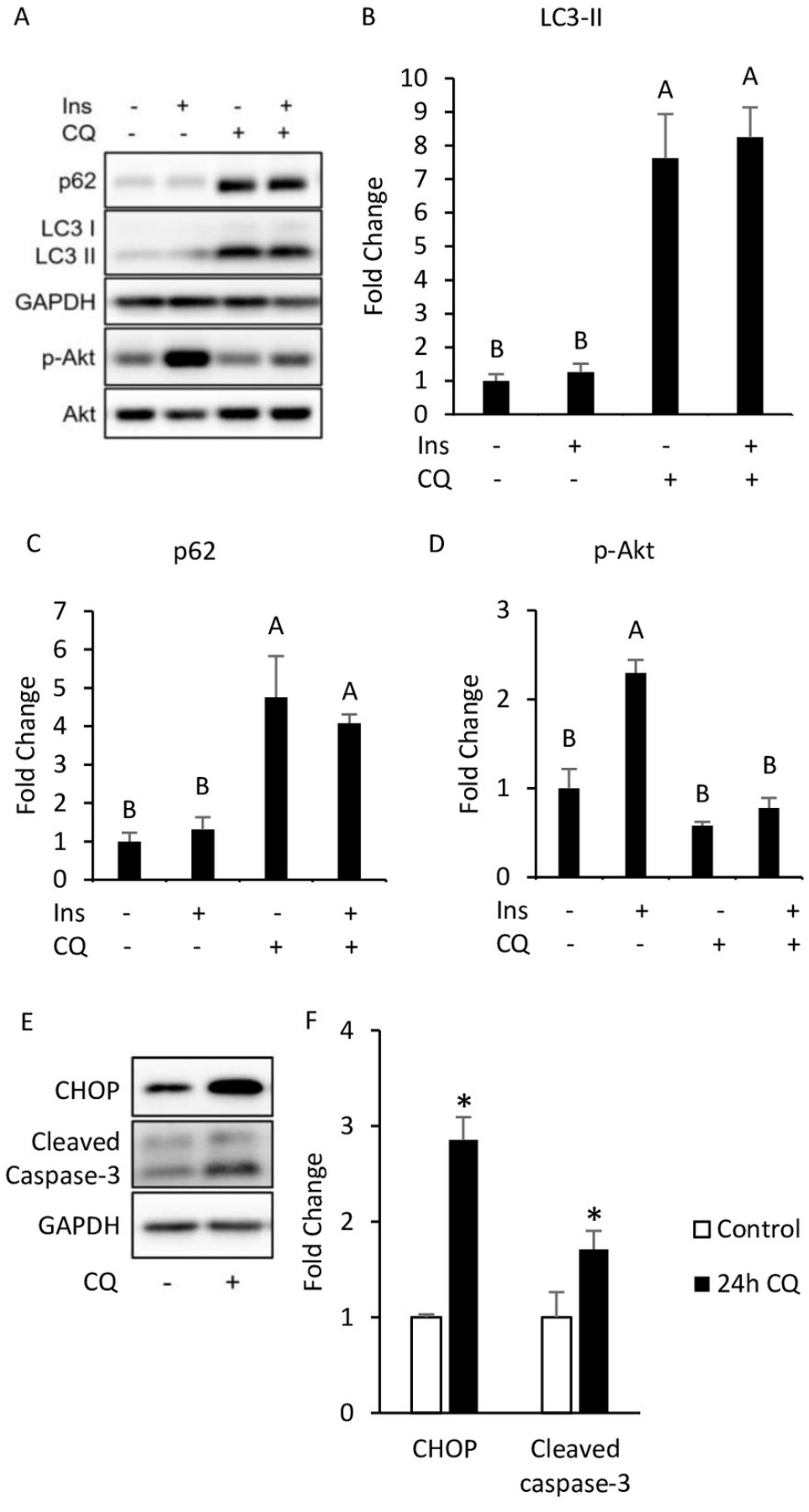
A
Ins - + - +
CQ - - + +
p62
LC3 I
LC3 II
GAPDH
p-Akt
Akt
B
LC3-II
Fold Change
10
9
8
7
6
5
4
3
2
1
0
B
B
A
A
Ins - + - +
CQ - - + +
C
p62
Fold Change
7
6
5
4
3
2
1
0
B
B
A
A
Ins - + - +
CQ - - + +
D
p-Akt
Fold Change
3
2
1
0
B
A
B
B
Ins - + - +
CQ - - + +
E
CHOP
Cleaved
Caspase-3
GAPDH
CQ - +
F
Fold Change
4
3
2
1
0
*
*
CHOP
Cleaved
caspase-3
Control
24h CQ

Figure 5

The insulin signaling pathway after chloroquine (CQ) treatment for 10 hours and 24 hours.

The insulin signaling pathway after chloroquine (CQ) treatment for 10 hours and 24 hours. B6 mice were injected with PBS or CQ into epididymal adipose tissue for 10 hours (A,B) and 24 hours (C,D,E) mice injected with or without I.P. insulin (0.5 IU/kg body weight, 30 minutes) before sacrifice. The phospho-Akt (Ser473) and total Akt levels of adipose tissues were analyzed with Western blotting. Blotting and quantitative data of p-Akt/Akt and p-GSK3β/ GSK3β were presented. Values are mean ± SEM (n=4) (A) (n=6) (C). Different letters are considered statistically significant difference by one-way ANOVA and least significant difference (LSD) test, $P < 0.05$. GAPDH was used as the loading control. The LC3B mRNA level in 24-hour PBS- and CQ-treated adipose was measured using qPCR analysis. For data quantification, the housekeeping gene ACTB was used as the internal control. Values are mean ± SEM (n=6). * indicates statistical significance, $P < 0.05$. n.s.: no significant difference.

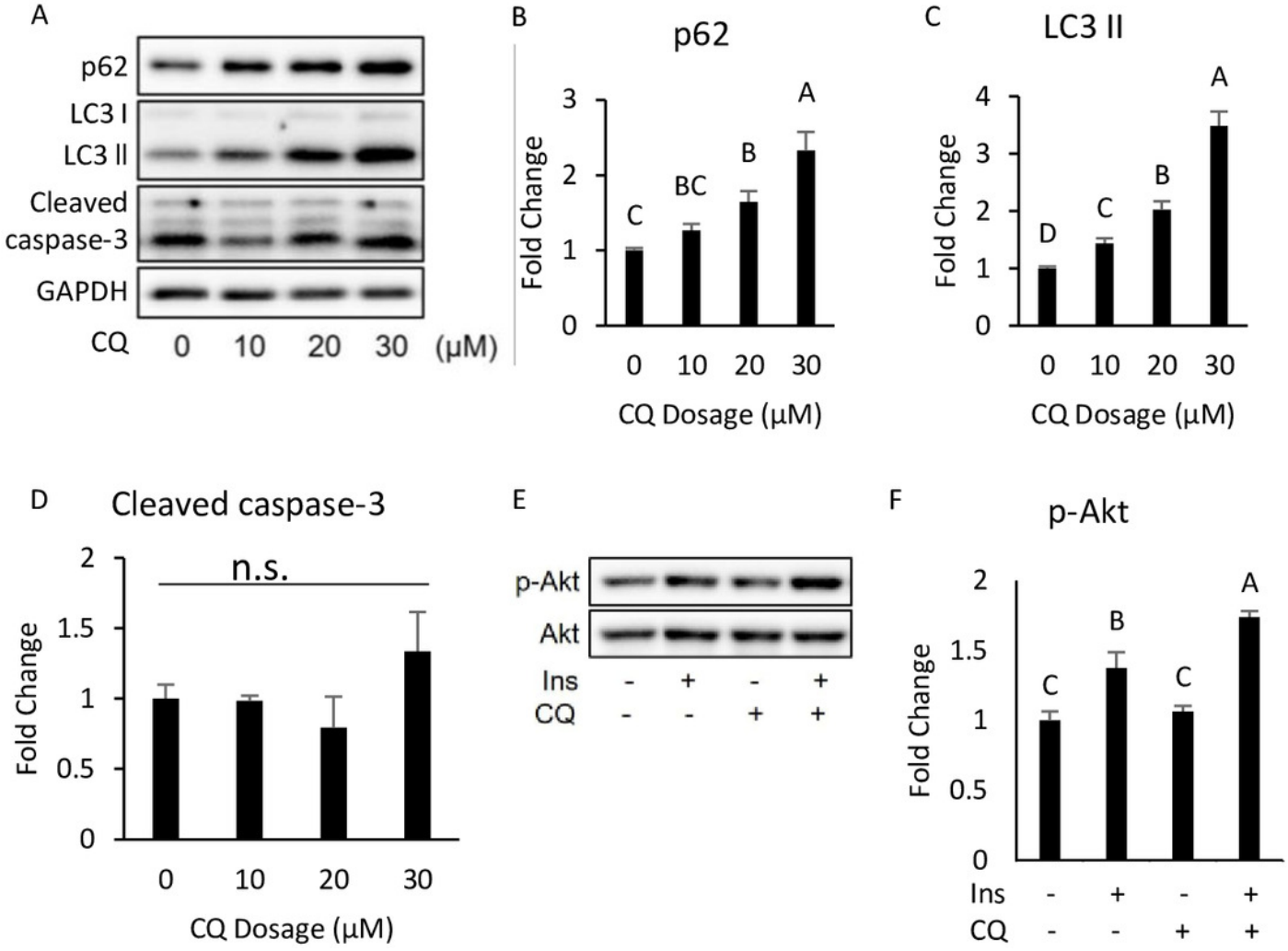
A
p62
LC3 I
LC3 II
Cleaved caspase-3
GAPDH
CQ 0 10 20 30 (μM)
B
p62
Fold Change
C BC B A
CQ Dosage (μM)
C
LC3 II
Fold Change
D C B A
CQ Dosage (μM)
D
Cleaved caspase-3
n.s.
Fold Change
CQ Dosage (μM)
E
p-Akt
Akt
Ins - + - +
CQ - - + +
F
p-Akt
Fold Change
C B C A
Ins - + - +
CQ - - + +

Figure 6

The suppression of late-stage autophagy may have feedback effect which resulted in reduced mRNA level of LC3B

The suppression of late-stage autophagy may have feedback effect which resulted in reduced mRNA level of LC3B. B6 mice were injected with PBS or CQ into epididymal adipose tissue for 24 hours. Representative SQSTM1/p62 and LC3 immunoblots and densitometric quantifications (A,B). For densitometric analyses of Western blotting data, GAPDH was used as loading control. The LC3B mRNA level in 24-hour PBS- and CQ-treated adipose was measured using qPCR analysis (C). For data quantification, the housekeeping gene ACTB was used as the internal control. Values are mean ± SEM (n=6). * indicates statistical significance, $P < 0.05$. n.s.: no significant difference.

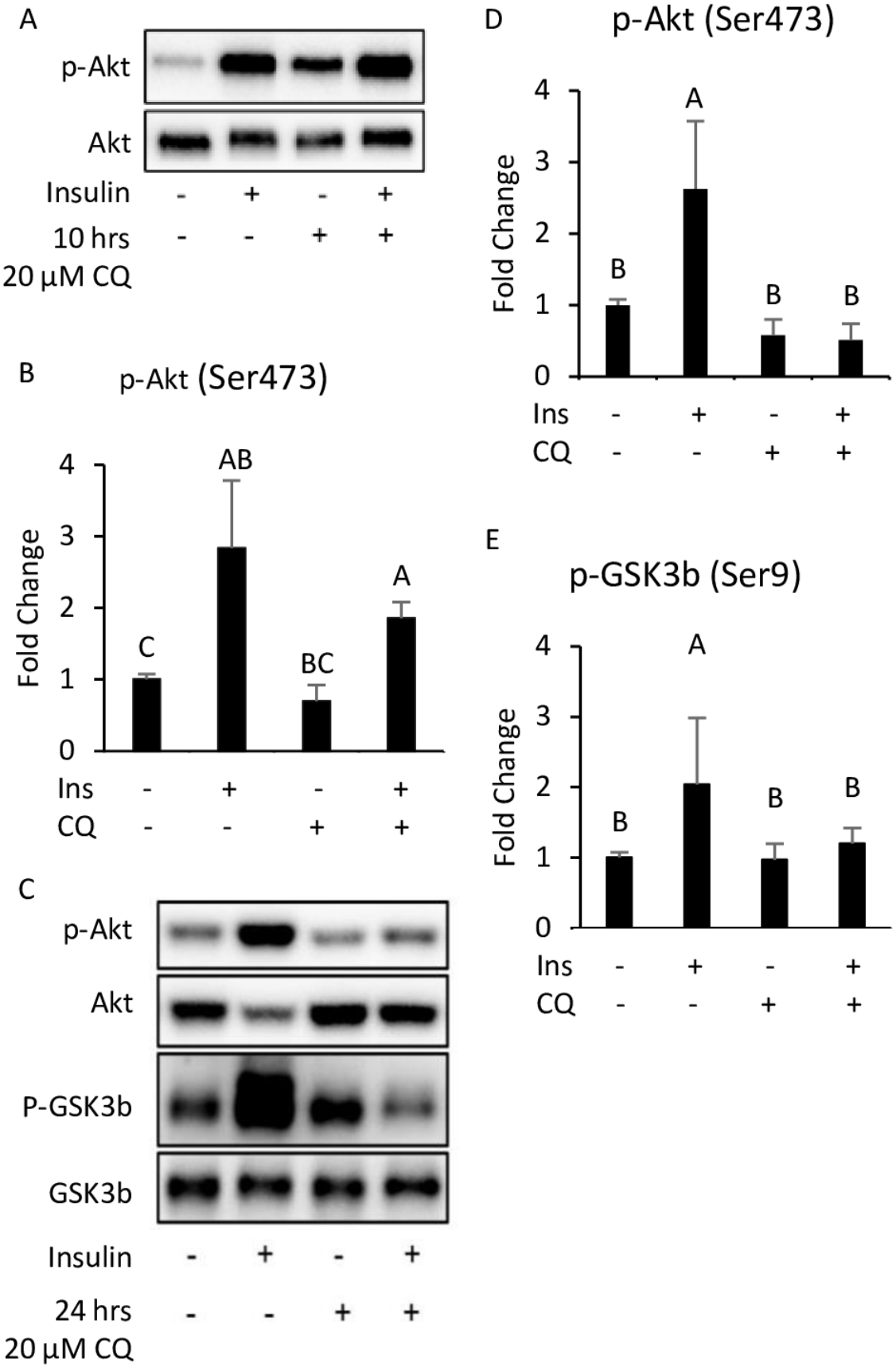
A
p-Akt
Akt
Insulin - + - +
10 hrs - - + +
20 µM CQ
B
p-Akt (Ser473)
Fold Change
4
3
2
1
0
C
AB
BC
A
Ins - + - +
CQ - - + +
C
p-Akt
Akt
P-GSK3b
GSK3b
Insulin - + - +
24 hrs - - + +
20 µM CQ
D
p-Akt (Ser473)
Fold Change
B
A
B
B
Ins - + - +
CQ - - + +
E
p-GSK3b (Ser9)
Fold Change
B
A
B
B
Ins - + - +
CQ - - + +

Figure 7

Autophagy may regulate insulin-stimulated signal transduction without associated with PHLPP1 and PTEN

Autophagy may regulate insulin-stimulated signal transduction without associated with PHLPP1 and PTEN. The PHLPP1 and PTEN level of PBS- and CQ-injected mouse adipose via Western blotting. * indicates statistical significance, P <0.05. Western blotting and quantitative data of PTEN were presented. For densitometric analyses of Western blotting data, GAPDH was used as the loading control. Values are mean ± SEM (n=3). n.s.: no significant difference.

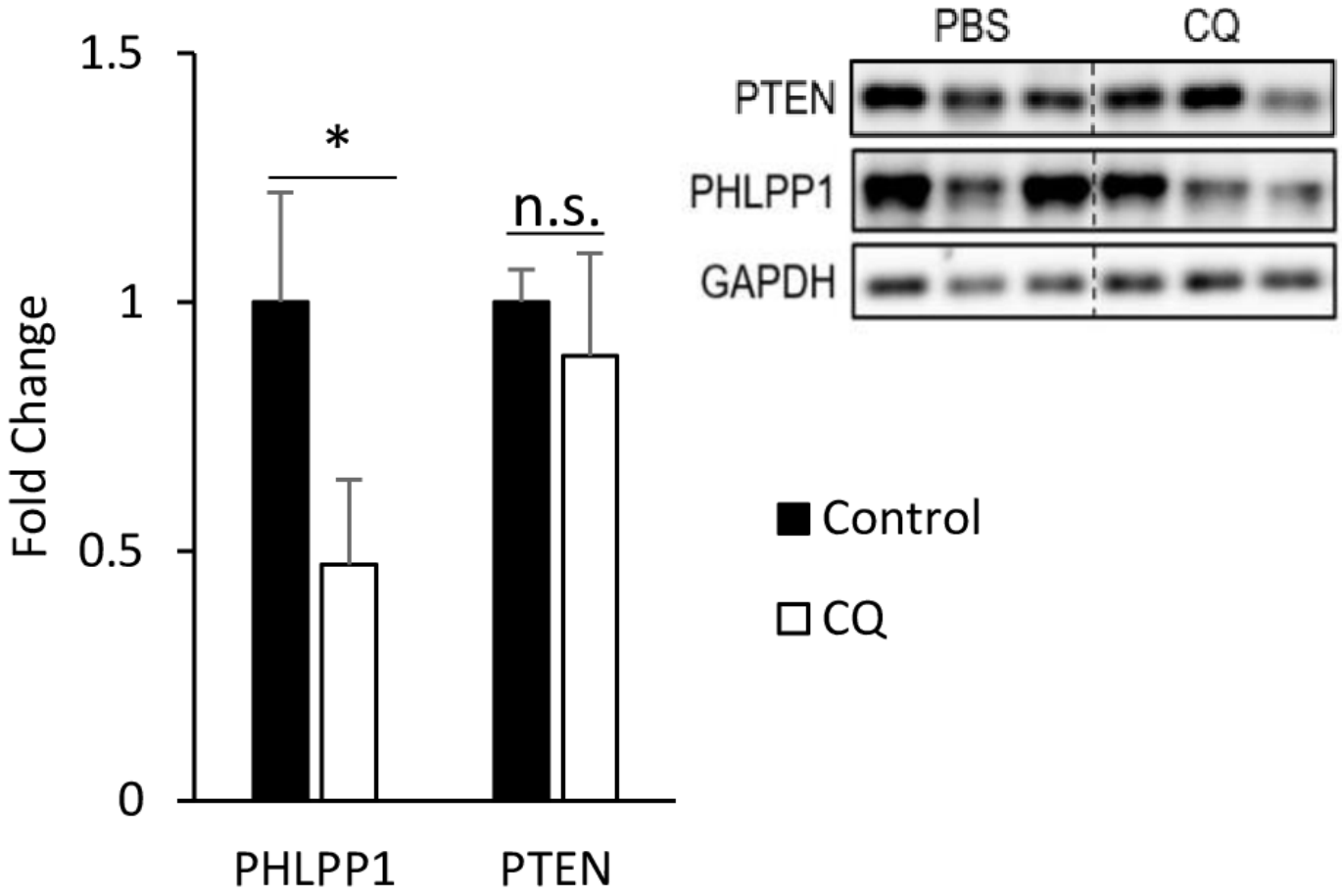

Table 1(on next page)

The antibodies used in the study

Table 1. The antibodies used in the study

Antibody Name	Company Product	Number
Anti-Akt	Cell Signaling Technology	4691S
Anti-phospho-Akt Ser 473	Cell Signaling Technology	4060S
Anti-ATG5	Cell Signaling Technology	12994S
Anti-CHOP	Cell Signaling Technology	2895S
Anti-cleaved caspase 3	Cell Signaling Technology	9664S
Anti-GAPDH	Cell Signaling Technology	2118S
Anti-GSK-3β	Cell Signaling Technology	3915S
Anti-phospho-GSK-3β S9	Cell Signaling Technology	5558S
Anti-LC3	Cell Signaling Technology	2775S
Anti-PHLPP1	Merck Millipore	07-1341
Anti-PTEN	Cell Signaling Technology	9559S
Anti-Rubicon	Cell Signaling Technology	8465S
Anti-SQSTM1/p62	Abcam	ab109012
Goat anti-rabbit IgG-HRP	Santa Cruz Biotechnology	sc-2004

Table 2(on next page)

The primer pairs used in qPCR analysis

1 Table 2. The primer pairs used in qPCR analysis

Gene Name	Forward (5' to 3')	Reverse (5' to 3')
Map1lc3b	GGAGCTTTGAACAAAGAGTGGAA	GGTCAGGCACCAGGAACTTG
Actb	GTGCGTGACATCAAAGAG	CAAGAAGGAAGGCTGGAA

2

3